Nuclear Instruments and Methods in Physics Research A ▮ (▮▮▮▮) ▮▮▮–▮▮▮

Contents lists available at SciVerse ScienceDirect

Nuclear Instruments and Methods in Physics Research A

journal homepage: www.elsevier.com/locate/nima

Atomic layer deposited borosilicate glass microchannel plates for large area event counting detectors

O.H.W. Siegmund [a,*], J.B. McPhate [a], A.S. Tremsin [a], S.R. Jelinsky [a], R. Hemphill [a], H.J. Frisch [b], J. Elam [c], A. Mane [c], LAPPD Collaboration [c]

[a] Experimental Astrophysics Group, Space Sciences Laboratory, 7 Gauss Way, University of California, Berkeley, CA 94720, USA
[b] Enrico Fermi Institute, 5640 S. Ellis Avenue University of Chicago, Chicago, IL 60637, USA
[c] Argonne National Laboratory, 9700 S. Cass Avenue Argonne, IL 60439, USA

ARTICLE INFO

Keywords:
Photon counting
Microchannel plate
Imaging
GaN
Cherenkov
Bialkali

ABSTRACT

Borosilicate glass micro-capillary array substrates with 20 μm and 40 μm pores have been deposited with resistive, and secondary electron emissive, layers by atomic layer deposition to produce functional microchannel plates. Device formats of 32.7 mm and 20 cm square have been fabricated and tested in analog and photon counting modes. The tests show amplification, imaging, background rate, pulse shape and lifetime characteristics that are comparable to standard glass microchannel plates. Large area microchannel plates of this type facilitate the construction of 20 cm format sealed tube sensors with strip-line readouts that are being developed for Cherenkov light detection. Complementary work has resulted in Na_2KSb bialkali photocathodes with peak quantum efficiency of 25% being made on borosilicate glass. Additionally GaN (Mg) opaque photocathodes have been successfully made on borosilicate microchannel plates.

1. Introduction

As part of a collaborative program the University of California, Berkeley, the Argonne National Laboratory (ANL), the University of Chicago and other University and Industrial partners, are developing a 20 cm square sealed tube microchannel plate (MCP) detector [1]. Potential applications, including detection of Cherenkov light, require imaging, and good quantum efficiency and timing characteristics. One significant challenge is implementation of large area MCPs with low cost and good functionality. To address this we have been collaborating with INCOM Inc. to make MCPs using borosilicate glass micro-capillary array substrates [1]. Unlike conventional MCPs, the resistive and photo-emissive surfaces of the MCP are sequentially applied by atomic layer deposition (ALD) [2]. Progress in development of these devices has been rapid, with good overall results.

The conceptual design for a large area sealed tube assembly is shown in Fig. 1. A borosilicate Schott Borofloat 33 entrance window transmits incoming photons (>300 nm) and semi-transparent proximity focused (0.5 mm gap) bialkali photocathode converts photons to photoelectrons. A pair of MCPs (gain $\sim 3\times10^6$) amplifies the signal, which is then detected on a strip-line readout anode. The latter will give modest spatial resolution and should provide timing accuracy of a few picoseconds [1]. The Berkeley detector design (Fig. 1) uses standard brazing techniques with an alumina ceramic tube body, hot indium seal well and strip-line anode substrate (the Argonne National Laboratory design has a glass envelope [1]). All connections to internal parts are made using hermetically sealed brazed pins through the anode substrate and we have incorporated non-evaporable getters inside the tube to maintain high vacuum. Given the large size of the detector there are "X" shaped ceramic spacers to maintain the internal spacing ($\sim$0.5 mm between the MCPs, and $\sim$6 mm between the MCPs and anode) of components and to reduce the deformation of the window and anode under atmospheric pressure.

2. Borosilicate microchannel plate design

INCOM, Inc. has constructed MCP substrates with 40 μm pores (65% and 83% open area ratio, 60:1 channel length/diameter (L/D)) and 20 μm pores (65% open area ratio, 60:1 L/D) using borosilicate glass micro-capillary arrays. Beginning with hollow tubes, the MCP substrates are made by a furnace drawing/stacking/fusing/slicing/and polishing process. Both the 32.7 mm round and 20 cm square substrates (Fig. 2) have 8° pore bias angle. The quality of substrates is now quite good, with no "triple point" stacking voids and minimal blocked pores [3]. The hexagonal multi-fiber boundaries are still seen (Fig. 2) due to the

* Corresponding author. Tel.: +1510 642 0895; fax: +1510 643 9729.
E-mail address: ossy@ssl.berkeley.edu (O.H.W. Siegmund).

0168-9002/$ - see front matter © 2011 Elsevier B.V. All rights reserved.
doi:10.1016/j.nima.2011.11.022

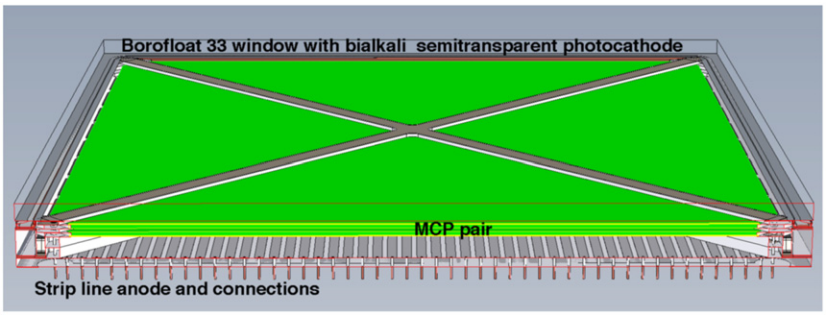

Fig. 1. Cut-away section of a model for a 20 cm sealed tube detector. The entrance window is borosilicate with a semi-transparent bialkali photocathode on the inner surface. Photoelectrons emitted by the photocathode are multiplied by a borosilicate substrate MCP pair that are functionalized using atomic layer deposition. The resulting electron clouds are then deposited onto a strip-line anode for position and arrival time determination.

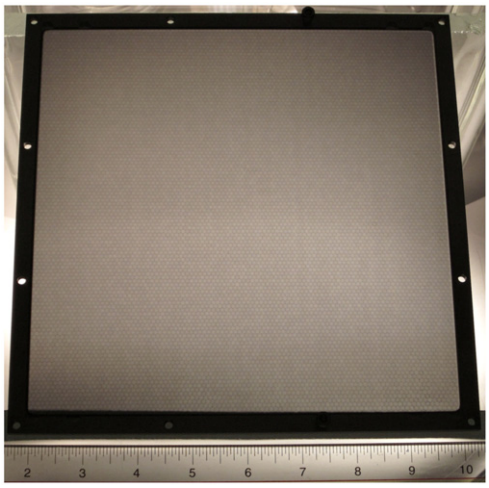

Fig. 2. Photograph of a 20 cm × 20 cm MCP made using ALD treatment of a borosilicate glass micro-capillary array. 20 μm pores, L/D=60:1, pore bias 8°. The multifiber hexagonal boundaries are visible in this backlit image.

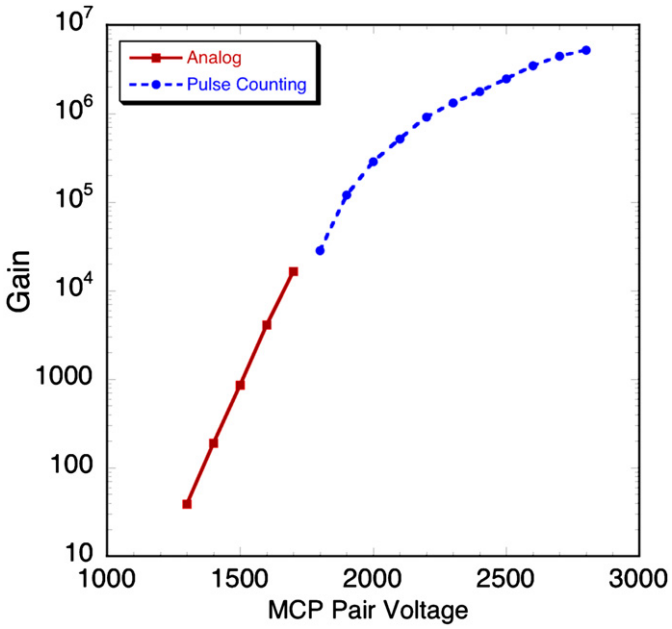

Fig. 3. Gain/voltage curve covering both photon counting and analog operation regimes for a pair of back to back 20 μm pore ALD coated borosilicate MCPs, L/D=60:1, pore bias 8°, 185 nm illumination.

deformation of a single row of pores at the interface, much like those seen in large area conventional glass MCPs made by ram fusion. Atomic layer deposition of resistive layers and secondary electron emissive layers on the surfaces of the substrates has been accomplished on 32.7 mm substrates by Arradiance, Inc. and at ANL. ANL has also done the ALD processes to produce 20 cm MCPs. The MCP resistances achieved cover a wide range from $<10\,\mathrm{M\Omega}$ to $>500\,\mathrm{M\Omega}$ accommodating all values seen for conventional glass MCPs.

3. Borosilicate microchannel plate tests

Detectors with either phosphor screen or cross delay line photon counting readouts have facilitated evaluations of borosilicate ALD MCPs. A significant number (>20) of 32.7 mm MCPs have been tested at this point and the results presented are representative of this data set. The gain (Fig. 3) for a back-to-back MCP pair shows similar characteristics to conventional MCPs [4] with evidence of gain saturation above 5×10^5 gain. The gain saturation is demonstrably seen by the achievement of peaked pulse amplitude distributions (Fig. 4), and is within expectations for MCP pairs [4]. Higher gain ($>3\times10^7$) has also been achieved when using a biased gap (0.7 mm, 300 V) between the two MCPs. Initial tests with a 20 cm square, 20 μm pore single MCP shows a gain–voltage curve, and current–voltage characteristic, that is essentially the same as the 32.7 mm test article MCPs.

Initial imaging tests were done using single MCPs with a phosphor screen readout and UV illumination (185 nm). The images (Fig. 5) show a uniform overall response with sharply defined MCP multifiber boundaries, and a small number of dark spot defects. This is considerably improved over prior results [3] where the substrates had a considerably larger incidence of defects. Images with pairs of MCPs and the cross delay line readout detector (Fig. 6) show two sets of multifiber patterns, a strong modulation from the top MCP, and a fainter modulation due to the bottom MCP. From the photon gain data we determine that in both cases the multifiber boundaries show lower gain than the surrounding areas, as might be expected from the pore crushing that occurs at these locations. The bright edge effect seen is due to optical and electronic reflections from the MCP mounting hardware. However, the overall response uniformity is reasonable ($\pm10\%$), with small variations caused by slight variations in the pore size.

The background rate for the newest MCPs is quite uniform (Fig. 7), and less than 0.1 event $\mathrm{cm^{-2}\,s^{-1}}$. This is less than conventional MCPs [4], and is expected since the radioactive emission from alkali metal isotopes is significantly reduced for borosilicate glass compositions compared with normal MCP lead glass. Measurements of MCP pulse shapes show Gaussian profiles with widths of the order 1 ns for a 20 μm pore MCP pair.

Please cite this article as: O.H.W. Siegmund, et al., Nuclear Instruments & Methods In Physics Research Section A (2011), doi:10.1016/j.nima.2011.11.022

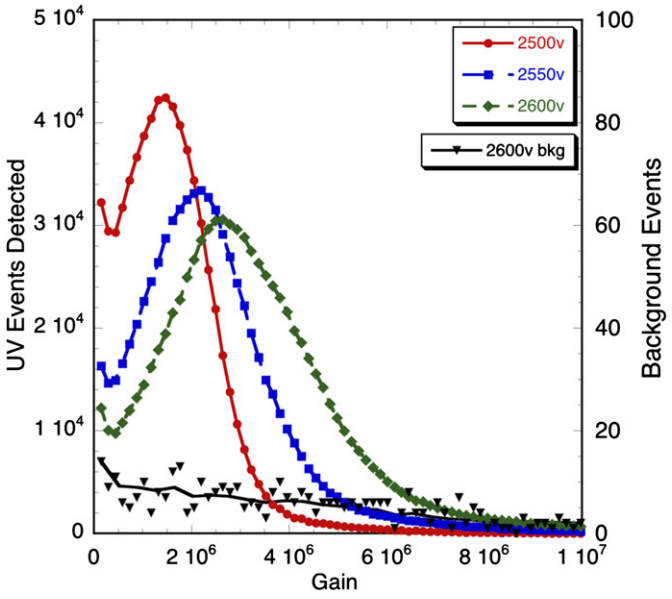

Fig. 4. Pulse height distributions for a pair of back to back 20 μm pore ALD coated borosilicate MCPs, L/D=60:1, pore bias 8°, 185 nm illumination. 1000 s background. Voltage applied=MCP pair voltage+400 V on anode gap.

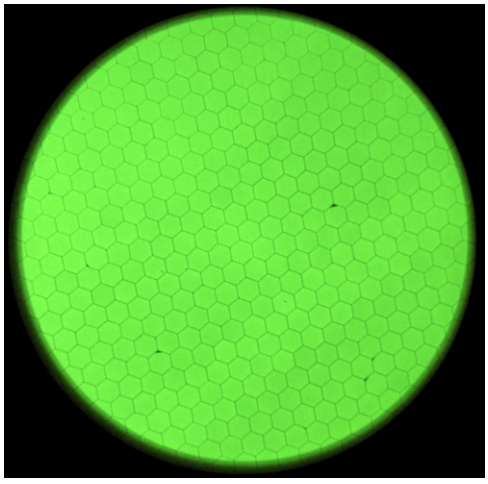

Fig. 5. Image for 185 nm UV illumination onto an ALD coated borosilicate MCP with 20 μm pores, L/D=60:1, pore bias 8°, $\sim 10^4$ gain, using a phosphor screen readout. The hexagonal multi-fiber packing structure is clearly visible, along with a few small MCP structural defects (dark spots).

We have also performed preconditioning (vacuum baking and operational burn-in) [5] of a borosilicate ALD MCP pair. A back to back MCP pair was tested in a high temperature compatible (ceramic/metal) cross delay line detector, then vacuum ($< 10^{-5}$ Torr) baked (350 °C) while monitoring the vacuum with a residual gas analyzer. The principal out-gas species were water vapor, hydrogen and standard atmospheric gases, and the partial pressures reduced by about an order of magnitude after bake. Post-bake gain and performance characteristics were essentially unchanged from their pre-bake values. The subsequent operational burn-in was done with uniform 185 nm illumination at a MCP gain of $\sim 10^4$ with about 1 μA output current. The relative gain trend shows a rapid drop (gas desorption) in the first 0.1 coulombs extracted, followed by a slow stabilization (Fig. 8). Compared with conventional MCPs tested under equivalent conditions, the trends are very similar. The principal gas evolved during burn-in was hydrogen, and its elimination is important to

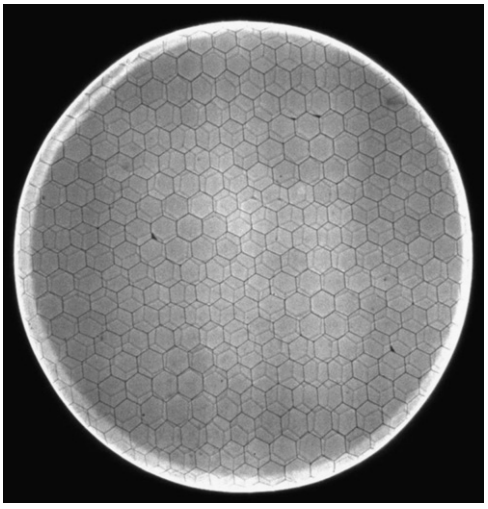

Fig. 6. Photon counting image (8×10^7 photons, 1024×1024 pixels, XDL readout) under 185 nm UV illumination using a gapped (0.7 mm, 300 V) pair of ALD coated borosilicate MCPs with 20 μm pores, L/D=60:1, pore bias 8° and 1.2×10^7 gain. The hexagonal multi-fiber packing structure for both MCPs is clearly visible.

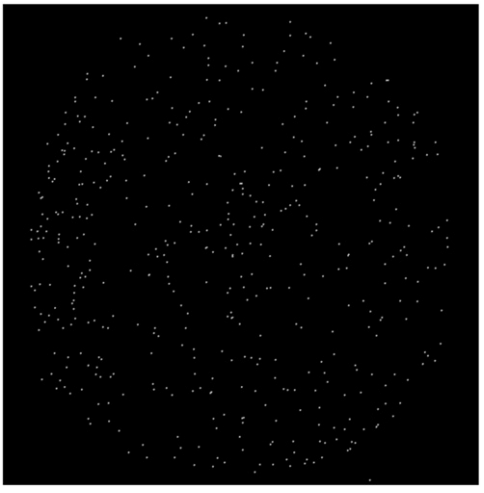

Fig. 7. Image of background event spatial distribution for a back-to-back pair of ALD coated borosilicate MCPs with 20 μm pores, L/D=60:1, pore bias 8°, 25 mm active area, 1000 s accumulation, 2.5×10^6 gain, 1100 V per MCP. Background rate 0.096events cm^{-2} s^{-1}.

MCP applications in sealed tubes to enhance photocathode lifetimes.

4. Photocathode development

In parallel with the MCP development we have deposited a number of bialkali photocathodes on borosilicate window samples to verify that reasonable quantum efficiency, stable photocathodes can be achieved. Several Na_2KSb photocathode depositions were accomplished using a co-evaporation method at high vacuum $< 10^{-7}$ Torr, as we would do for vacuum transfer device fabrication. In each case four 31 mm diameter Borofloat 33 disks were deposited at the same time, arranged within a 75 mm circle to evaluate photocathode uniformity. Prior to deposition the substrates were chemically cleaned and in-situ vacuum baked to 350 °C. An example of the quantum efficiency is shown in Fig. 9, measured using monochromatic LEDs and calibrated with a NIST standard photodiode. The peak Na_2KSb photocathode efficiency is good [6], with characteristic wavelength dependence for

Please cite this article as: O.H.W. Siegmund, et al., Nuclear Instruments & Methods In Physics Research Section A (2011), doi:10.1016/j.nima.2011.11.022

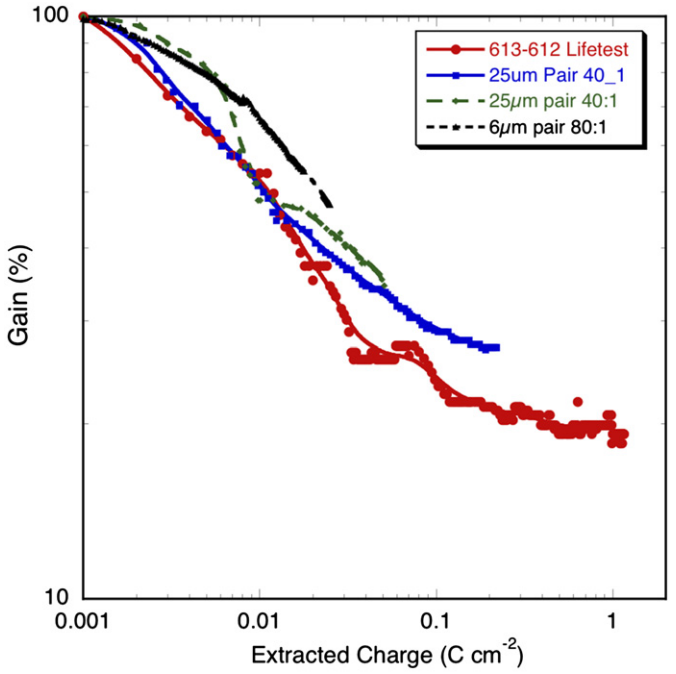

Fig. 8. Gain as a function of extracted charge for a back-to-back pair of ALD coated borosilicate MCPs (#613 on #612) with 20 μm pores, L/D=60:1, pore bias 8°, 25 mm active area (UV 185 nm flood) compared with the equivalent data for conventional MCP pairs.

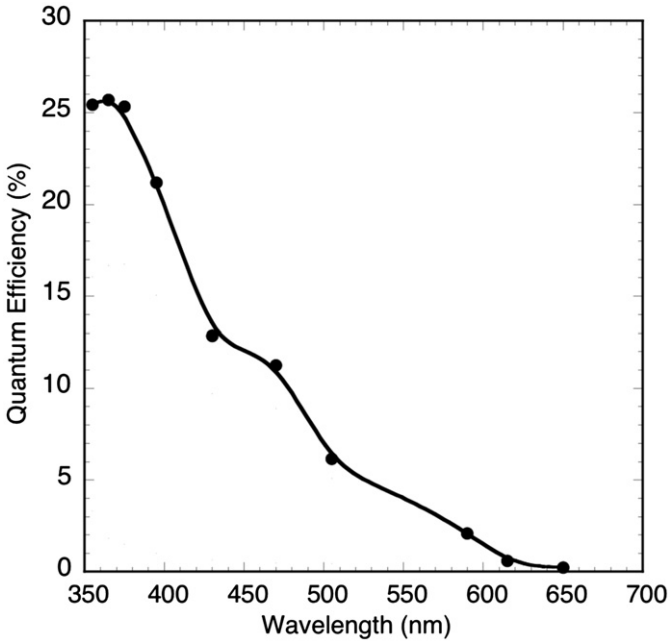

Fig. 9. Measurements of the quantum efficiency of a Na_2KSb photocathode deposited onto a borofloat 33, 31 mm diameter test window.

this type of photocathode. The quantum efficiency uniformity over the substrates was found to be better than 10%, and they were stable over the time period that they were kept under high vacuum (~1 week).

We have also deposited GaN (Mg) photocathode material directly onto the NiCr electrode layer of borosilicate ALD MCPs. The deposition was done by molecular beam epitaxy (by SVT Associates Inc.) onto a 32.7 mm MCP in "pie-section" zones of different thicknesses of 100 nm, 300 nm, 700 nm, 900 nm and 1000 nm. Measurements under UV illumination in a detector with a cross delay line readout show significant enhancement of the QE, with clearly defined imaging of the zone boundaries. This is evident both before and after Cs treatment comparing with the bare uncoated NiCr zone. After Cs activation the measured QE (using 214 nm UV) of the top surface "web" area of the MCP increases from ~5% for the 100 nm zone to ~10% for the 300 nm and thicker zones. This trend is as expected for opaque photocathodes, but the QE is significantly less (÷4) than has been achieved on sapphire substrates [7]. Given the non-optimal substrate lattice matching conditions, however, this QE is quite encouraging. We propose to use an Al_2O_3 pre-deposition layer for future tests to improve the layer interface conditions.

5. Conclusions

Optimization of borosilicate/ALD 32.7 mm MCPs shows significant progress, and display operational characteristics much like conventional MCPs in both analog and photon counting configurations. Large format 20 cm MCPs are now available and initial tests suggest they function similarly. Bialkali photocathodes of high QE have also been made on representative borosilicate windows. Thus the most critical components are in good stead for the implementation of a large area sealed tube detector.

Acknowledgments

We wish to thank the members of the team at INCOM, Inc., Arradiance Inc., Mr. J. Hull, and Mr. J. Tedesco for their contributions to this work. This work was supported by DOE/Argonne under contract DE-AC02-06CH11357.

References

[1] M. Wetstein, on behalf of the LAPPD collaboration, Nuclear Instruments and Methods 639 (1) (2011) 148.
[2] M. Ritala, M. Leskelä, Nanotechnology 10 (1) (1999) 19.
[3] O.H.W. Siegmund, J.B. McPhate, J.V. Vallerga, A.S. Tremsin, S.R. Jelinsky, H.J. Frisch, and the LAPPD collaboration, Nuclear Instruments and Methods 639 (1) (2011) 165.
[4] O.H.W. Siegmund, Methods of Vacuum Ultraviolet Physics, Chapter III, second ed., in: J.A.R. Samson, D.L. Ederer (Eds.), Academic Press, 1998.
[5] O.H.W. Siegmund, Proceedings of SPIE 1072 (1989) 111.
[6] C. Ghosh, B.P. Varma, Journal of Applied Physics 49 (8) (1978) 4549.
[7] O.H.W. Siegmund, J.S. Hull, A.S. Tremsin, J.B. McPhate, A. Dabiran, SPIE 7732 (2010) 77324T.